

# Superelliptical laws for complex networks

Stefano Allesina<sup>\*1,2</sup>, Elizabeth Sander<sup>1</sup>, Matthew J. Smith<sup>1</sup>, and Si Tang<sup>1</sup>

<sup>1</sup>Department of Ecology & Evolution, University of Chicago

<sup>2</sup>Computation Institute, University of Chicago

May 25, 2022

## Abstract

All dynamical systems of biological interest—be they food webs, regulation of genes, or contacts between healthy and infectious individuals—have complex network structure. Wigner’s semicircular law and Girko’s circular law describe the eigenvalues of systems whose structure is a fully connected network. However, these laws fail for systems with complex network structure. Here we show that in these cases the eigenvalues are described by superellipses. We also develop a new method to analytically estimate the dominant eigenvalue of complex networks.

Eigenvalues and eigenvectors are central to science and engineering. They are used to assess the stability of dynamical systems[1], the synchronization of networks[2], the occurrence of epidemics of infectious diseases[3, 4, 5, 6, 7], and the ranking of web-pages[8].

Two connected results describe the eigenvalue distribution of large matrices with random coefficients: Wigner’s semicircle law[9] (for symmetric matrices), and Girko’s circular law[10] (for asymmetric ones).

These laws have been applied in a wide range of disciplines, from number theory[11] to ecology[1]. However, they fall short of describing the eigenvalues of matrices with complex network structure[12]. Such matrices are ubiquitous in the analysis of man-made and biological systems[13, 14].

Here we analyze matrices whose underlying structure is a sparse random network with arbitrary degree distribution. We show that the eigenvalue distributions of these matrices are described by superellipses. We solve the case of symmetric matrices by generalizing Wigner’s law, and extend Girko’s law to matrices with regular-graph structure (where all nodes have the same degree). We also propose a new method to approximate the dominant eigenvalue of a complex network, improving upon current results[15, 16].

Wigner’s semicircle law[9] states that the density of the eigenvalues of a large, symmetric random matrix whose entries are sampled from a normal distribution  $\mathcal{N}(0, \sigma^2)$  is described by a semicircle. Similarly, Girko’s circular law[17, 10, 18] states that the eigenvalues of asymmetric matrices with normally-distributed entries are approximately uniformly distributed in a circle. If there is a nonzero pairwise correlation between the off-diagonal elements of the matrix, the eigenvalues are approximately uniformly distributed in an ellipse[19, 20, 21]. These laws have found applications in a wide array of disciplines, including quantum physics[22], ecology[1] and number theory[11], and were recently proved to be universal[18, 21] – i.e., they hold under very mild conditions on the distribution of the matrix entries.

Wigner’s and Girko’s laws hold for matrices whose underlying network structure is a completely connected graph: as  $s$ , the size of the graph, goes to infinity, the distribution of the eigenvalues converges to the corresponding law. They also hold for not-completely-connected graphs[18], as long as the number of connections per node  $sp$  (where  $p$  is the proportion of nonzero entries in the matrix) goes to infinity as  $s \rightarrow \infty$ .

However, the laws do not describe the eigenvalues of matrices with complex network structure[12]. These networks are typically sparse with a very heterogeneous degree distribution[14]; moreover, for most complex networks, we expect the average number of connections per node to approach a constant as the network grows[12]. In this case, as  $s \rightarrow \infty$ ,  $sp \rightarrow k$ . The cap on the average number of connections per node

---

\*sallesina@uchicago.edu

can arise from spatial or temporal constraints. For example, in an ecological system organisms need to spatiotemporally co-occur in order to interact. The cap is also evident in empirical data: Facebook counted around 56 million active users in 2008[23], each with an average degree (number of friends) of about 76, and while the number of users grew to more 562 million in 2011, the average degree grew only to 169.

Our goal is to extend the circular laws above to the case of large matrices with complex network structure, whose average degree is  $k \ll s$ . We show that in such cases the eigenvalue distributions are described by superellipses ( $|x|^n/a^n + |y|^n/b^n \leq 1$ , where  $x$  is the real part of an eigenvalue and  $y$  is its imaginary part; for  $n = 2$ , we recover the equation for an ellipse).

For symmetric matrices with normally-distributed entries (the analog of Wigner’s case), the density of the eigenvalues is described by a semi-superellipse – for any degree distribution of the underlying network. For asymmetric matrices (Girko’s case) whose structure is a random  $k$ -regular graph (i.e., all nodes have the same degree), we find that the eigenvalues are approximately uniformly distributed in a superellipse. For other network structures, the distribution is still described by superellipses, but is not uniform.

## Results

### Symmetric Matrices

We analyze  $s \times s$  matrices with 0 on the diagonal, and off-diagonal pairs  $(M_{ij}, M_{ji})$  obtained by multiplying the corresponding entries of two matrices  $(M_{ij}, M_{ji}) = (A_{ij}, A_{ji}) \cdot (N_{ij}, N_{ji})$ .  $A$  is the adjacency matrix of a random undirected graph—with a given degree distribution—built using the configuration model[24, 14]. The use of the configuration model is important, as it ensures that the networks do not typically have unwanted “secondary structures” (e.g., modules, bipartite or lattice structure) that would affect results.  $N$  is a matrix whose off-diagonal pairs  $(N_{ij}, N_{ji})$  are sampled from a bivariate normal distribution  $(X, Y)$ , with  $\mathbb{E}[X] = \mathbb{E}[Y] = 0$ ,  $\mathbb{E}[X^2] = \mathbb{E}[Y^2] = 1/k$ , and  $\mathbb{E}[XY] = \rho/k$ , where  $k$  is the average degree of the network and  $-1 \leq \rho \leq 1$  is Pearson’s correlation coefficient. The choice of parameters ensures that for  $k \rightarrow \infty$ , we recover the type of matrices studied by Wigner and Girko. Our results also hold for non-normal distributions (e.g., uniform, SI).

We start with the analog of Wigner’s case, in which matrices are symmetric ( $\rho = 1$ ). In this case, all eigenvalues are real, and for  $k \rightarrow \infty$  we recover Wigner’s semicircle probability distribution function:

$$\Pr(\lambda = x) = P(x) = \frac{2\sqrt{(2r)^2 - x^2}}{\pi(2r)^2} \quad (1)$$

The variance of this distribution is a function of  $r$ :  $\mu_2(r) = \int x^2 P(x) dx = r^2$ . Because the variance of the eigenvalues of a matrix with diagonal zero is  $\text{Tr}(M^2)/s = \rho = \mu_2(r)$ , given that in our matrices  $\rho = 1$ , then  $r = 1$  and thus the horizontal radius is  $a = 2r = 2$ . We next generalize Wigner’s formula to the case where  $k \ll s$ , which leads to a semi-superelliptical distribution:

$$P(x) = \frac{2\sqrt[n]{(2r)^n - x^n}}{4(2r)^2\Gamma(1 + 1/n)^2\Gamma(1 + 2/n)^{-1}} \quad (2)$$

where the numerator is the superelliptical equivalent of Wigner’s formulation, and the denominator is the area of a superellipse with  $a = b = 2r$ . In this case, we need to solve for two parameters,  $r$  and  $n$ . Hence, we write equations for the second ( $\mu_2(r, n) = \int x^2 P(x) dx = \text{Tr}(M^2)/s$ ) and fourth ( $\mu_4(r, n) = \int x^4 P(x) dx = \text{Tr}(M^4)/s$ ) central moments of the eigenvalue distribution ( $\mu_3(r, n) = 0$ , due to symmetry), thereby obtaining the values of  $n$  and  $r$  (SI).

In Figure 1, we show numerical simulations in which we take a single  $5000 \times 5000$  matrix, whose network structure is determined by the average degree  $k$  (columns) and a specific algorithm used to construct the degree distribution (rows). In all cases, the density of the eigenvalues is described by a semi-superellipse, which captures the tails especially well. This is important, given the role of dominant eigenvalues in determining the properties of dynamical systems. The distribution tends to underestimate (small  $k$ ) or overestimate (large  $k$ ) the number of zeros, especially for very skewed degree distributions – an effect similar to that found for small matrices in Girko’s circular law[18].

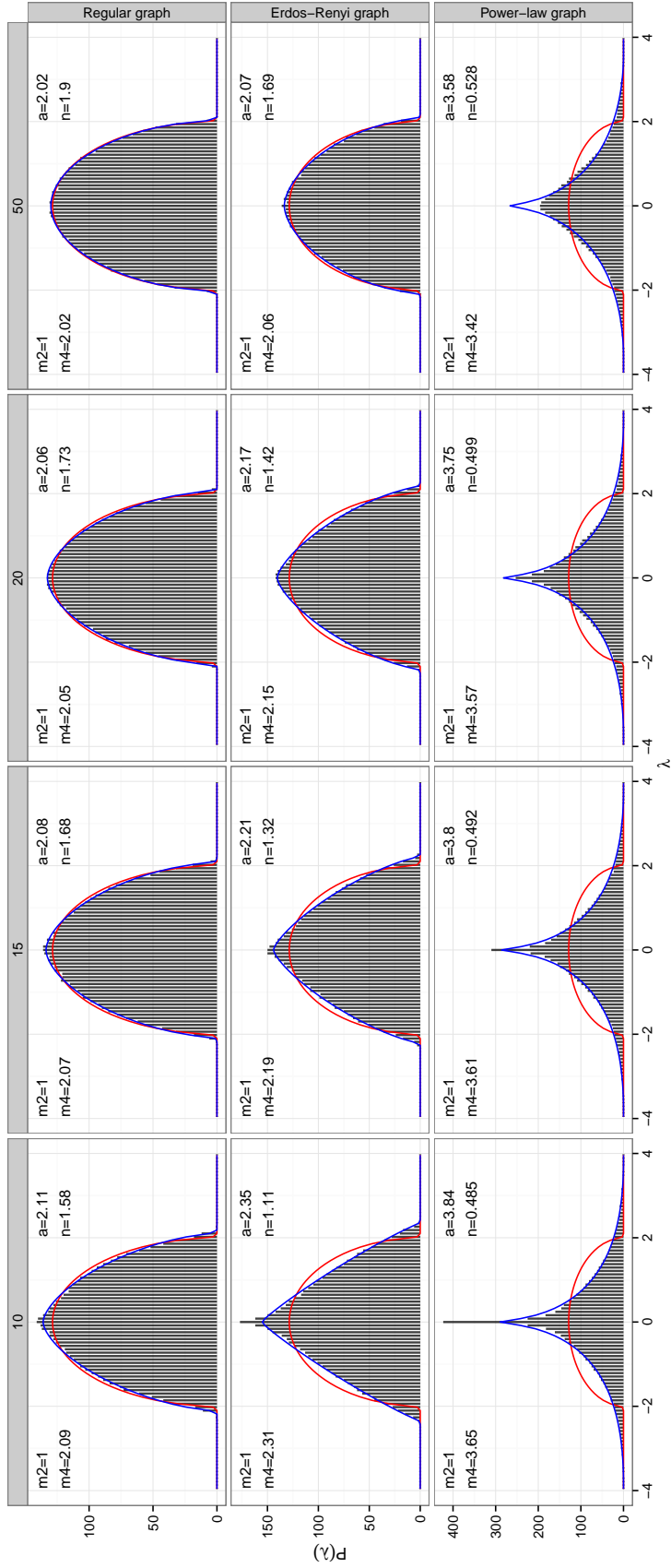


Figure 1: Probability density function for the eigenvalues of symmetric matrices whose underlying structure is a complex network. The network has average degree  $k$  (columns), and degree distribution determined by different algorithms (rows). For a given degree distribution, the network is then built using the configuration model [24, 14]. The values of the nonzero elements are sampled from a symmetric bivariate normal distribution centered at zero (SI). The red line marks the prediction of Wigner's semicircle distribution [9]. The blue line shows the semi-superelliptical distribution when  $\mu_2$  and  $\mu_4$  (top left in the panel) are used to solve the equations determining its parameters ( $a$  and  $n$  in the panels). Each graph is obtained by computing the eigenvalues of a single matrix of size  $5000 \times 5000$ .

## Asymmetric Matrices

We now move to the case in which  $\rho \neq 1$  (Figures 2 and 3). For  $k \rightarrow \infty$  and  $\rho = 0$ , we recover Girko's circular law, which states that the eigenvalues are uniformly distributed in the unit circle. For  $k \rightarrow \infty$  and  $-1 < \rho < 1$ , the eigenvalues are uniformly distributed in an ellipse with horizontal radius  $a = 1 + \rho$  and vertical radius  $b = 1 - \rho$ .

Although all the eigenvalue distributions appear to be described by superellipses in the complex plane, only matrices with  $k$ -regular graph structure have a distribution that is close to uniform. For these matrices, we can approximate the p.d.f. as:

$$\Pr(\Re(\lambda) = x, \Im(\lambda) = y) = P(x, y) = \frac{1}{4ab\Gamma(1 + 1/n)^2\Gamma(1 + 2/n)^{-1}} \quad (3)$$

Setting  $a = r(1 + \rho)$  and  $b = r(1 - \rho)$  (SI), we can replicate the approach above and write the second and fourth central moments as  $\mu_2(r, n) = \iint (x^2 - y^2)P(x, y)dydx = \text{Tr}(M^2)/s = \rho$  and  $\mu_4(r, n) = \iint (x^4 + y^4 - 6x^2y^2)P(x, y)dydx = \text{Tr}(M^4)/s$ , respectively. Solving these equations, we obtain  $n$  and  $r$  (SI).

## Adjacency Matrices

Many applications deal with matrices that do not comply with the strict requirements we set above. For example, adjacency matrices of undirected graphs have entries whose value is either zero or one. As such, the mean of the matrix is not zero, and thus the eigenvalues do not follow the semi-superellipse introduced above.

Consider a graph generated by the configuration model with arbitrary degree distribution: the density of all eigenvalues but the dominant one follows a semi-superellipse, while the dominant eigenvalue lies to the right of the semi-superellipse (SI). We can exploit this fact to accurately estimate the value of the dominant eigenvalue (Figure 4).

One notable characteristic of semi-superelliptical distributions is that they are symmetric about the mean. As such, the distribution obtained by taking all the eigenvalues but the dominant one should have odd central moments  $\tilde{\mu}_{2z+1} \approx 0$ . Hence, one can solve a system of equations of the form  $\text{Tr}(A^z) = \sum_j \lambda_j^z = (s - 1)\tilde{\mu}'_z + \lambda_1^z$  (where  $\tilde{\mu}'_z$  is the  $z^{\text{th}}$  raw moment of the distribution obtained removing the dominant eigenvalue) by assuming, for example, that  $\tilde{\mu}_3 = 0$  or that  $\tilde{\mu}_5 = 0$  (SI).

We contrast the two approximations obtained by setting the  $3^{\text{rd}}$  or  $5^{\text{th}}$  central moments to zero and the fantastically simple one proposed by Chung *et al.*[15],  $\lambda_1 \approx \overline{k^2/k}$  (i.e., the average of the squared degrees divided by the average degree). Chung's approximation holds as long as the minimum degree in the network is not too small compared to the mean degree, and was independently obtained by Nadakuditi & Newman[16] using free probability. Figure 4 shows that the approximation based on the fifth moment works better than the others for non-regular graphs.

## Discussion

A semi-superellipse approximates the density of the eigenvalues of the symmetric matrix  $M$ . When  $M$  is asymmetric, the eigenvalues fall in superellipses in the complex plane. When the structure of  $M$  is a random  $k$ -regular graph, then the distribution is approximately uniform and we can estimate the parameters of the superellipse.

The spectrum of the adjacency matrix of a random graph with arbitrary degrees can be described by a "semi-superellipse plus  $\lambda_1$ " distribution. Because a semi-superellipse is symmetric about the mean, we can analytically approximate the value of  $\lambda_1$ . This allows, for example, a more accurate prediction of the occurrence of epidemics in simple Susceptible-Infected-Susceptible and Susceptible-Infected-Recovered models that incorporate an explicit network of contacts between individuals[4, 3, 5, 6], for which the epidemic threshold is defined by  $1/\lambda_1$ .

Interestingly, we can connect the value of  $\lambda_1$  with the presence of small motifs[25] in the network. Our approximation of the dominant eigenvalue of adjacency matrices produced by the configuration model shows that the dominant eigenvalue of a network of a given size and connectivity strongly depends on the number of triangles (approximation using  $\tilde{\mu}_3$ ) and pentagons (using  $\tilde{\mu}_5$ ) it contains.

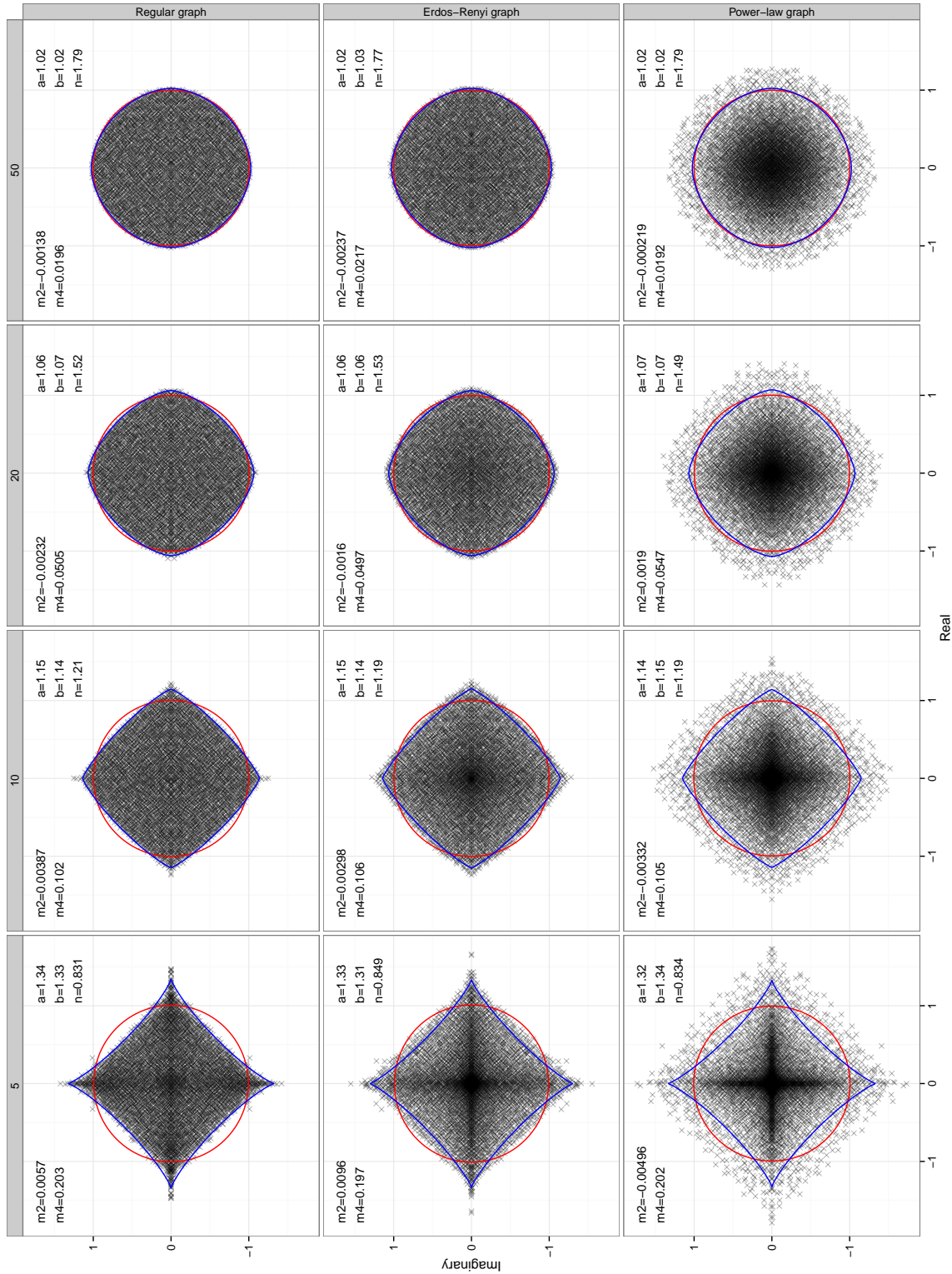


Figure 2: Distribution of the eigenvalues of asymmetric matrices ( $\mathbb{E}[\rho] = 0$ ) in the complex plane. As in Figure 1, the columns specify the average degree of the network, and the rows specify the algorithm used to build the degree distribution. The red line is obtained using Girko's circular law [17, 10, 18]. The blue line is obtained by solving for  $a$ ,  $b$  and  $n$  (top right in the panels) for the superelliptical distribution using the second and fourth moments of the eigenvalue distribution (top left in the panels). The superelliptical distribution is expected to accurately describe the case with  $k$ -regular graph structure, for which the eigenvalues are approximately uniform in the superellipse. Each graph is obtained computing the eigenvalues of a single matrix of size  $5000 \times 5000$ .

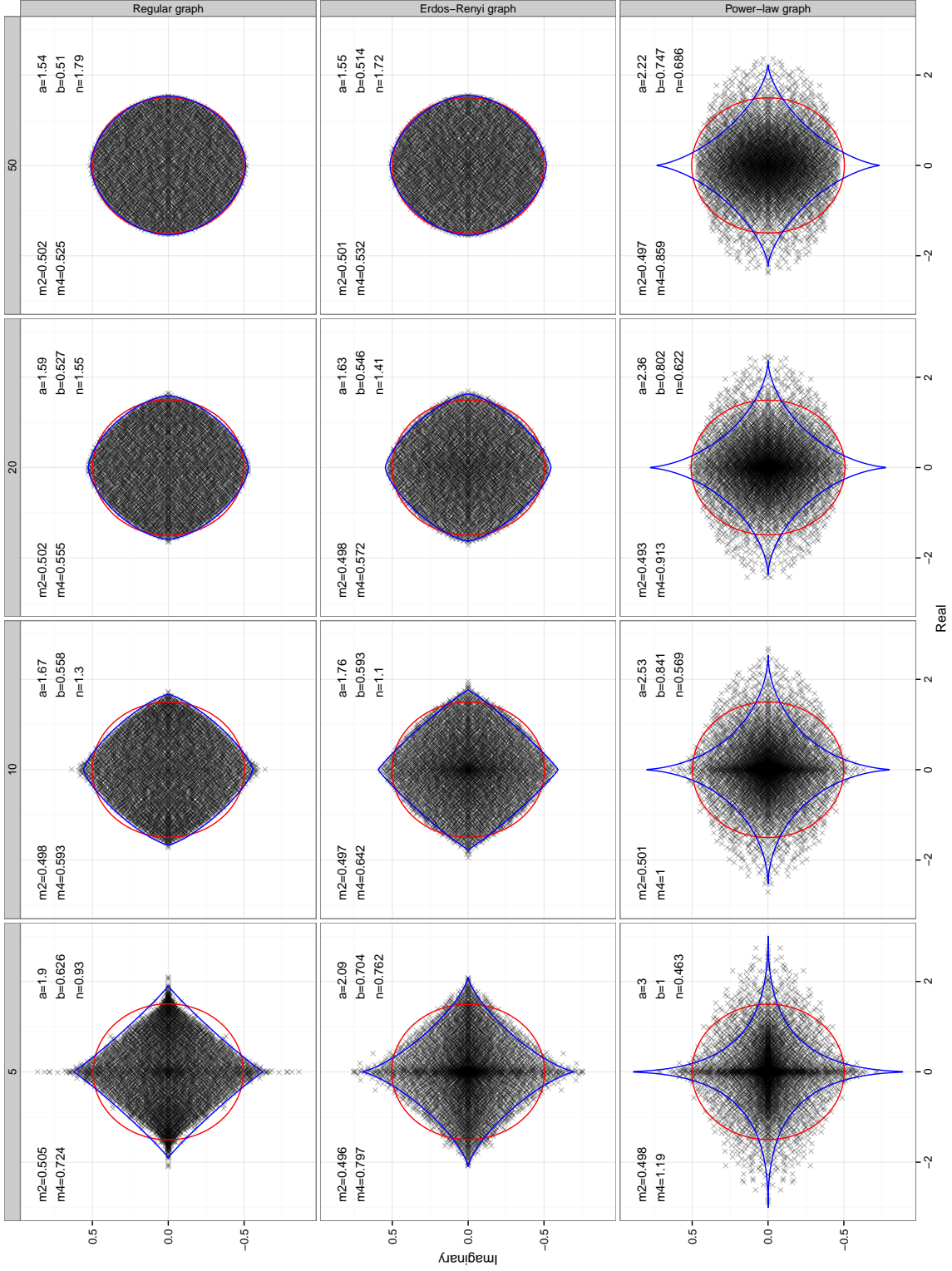


Figure 3: As Figure 2, but with positive correlation  $\mathbb{E}[\rho] = 0.5$ . In this case the red line describes the elliptical law [19, 20, 21].

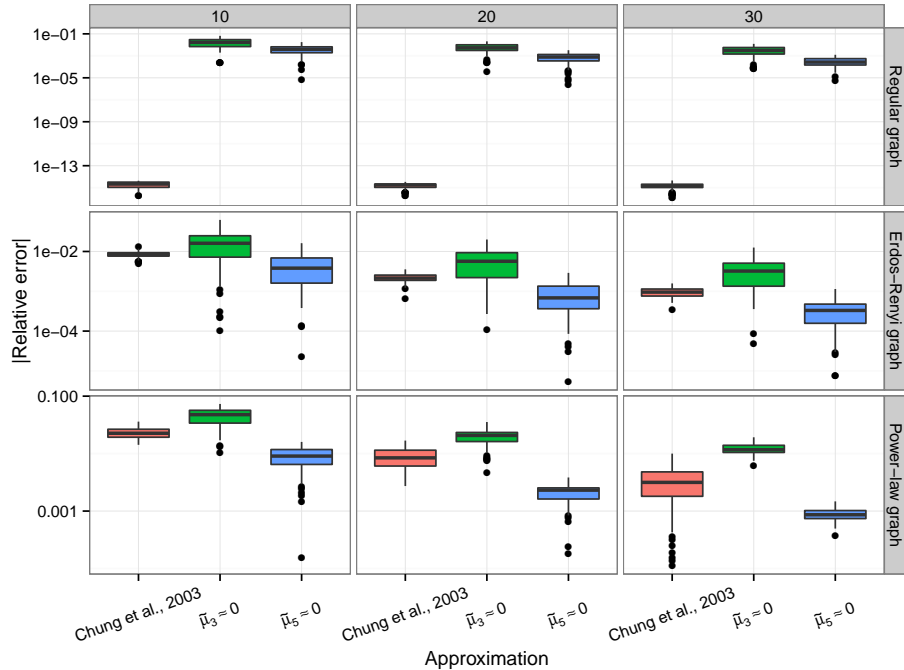


Figure 4: Approximation of the dominant eigenvalues of matrices built using the configuration model and choosing the degree distribution according to the algorithm specified in the rows. The columns stand for the desired average degree. The x-axis specifies the approximation used to obtain  $\lambda_1^{approx}$ , while the y-axis represents the absolute value of the relative error  $|(\lambda_1^{approx} - \lambda_1)|/|\lambda_1|$ .

We also considered departures from the configuration model (SI). We chose the configuration model in order to prevent the emergence of “secondary structures” in the network, but the ultimate test for these methods is to approximate the behavior of real, empirical networks, which are known to contain interesting structural features[14].

For symmetric matrices parametrized using the structure of networks of biological interest, the density of the eigenvalues is captured by the semi-superelliptical distribution. As expected, the asymmetric case is not well-described by the superelliptical distribution derived for  $k$ -regular graphs. Finally, in this case, the approximation of the dominant eigenvalue continues to perform very well, and better than current methods.

The results presented here open the door for the analytic study of large dynamical systems with complex network structure.

# Supporting Information

## List of symbols

For reference, we provide a list of the main symbols used in the following sections.

Symbol	Description
$\mathcal{N}(\boldsymbol{\mu}, \boldsymbol{\Sigma})$	Bivariate normal distribution with mean $\boldsymbol{\mu}$ and covariance matrix $\boldsymbol{\Sigma}$ .
$\mathbb{E}[X]$	Expectation of the random variable $X$ .
$\text{Var}[X]$	Variance of $X$ .
$\rho$	Pearson's correlation coefficient.
$\mathcal{U}(-t, t)$	Uniform distribution on the interval $[-t, t]$ .
$\mu'_z$	$z^{\text{th}}$ raw moment (moment about the origin) of a distribution. We sometimes write $\mu'_z(r, n)$ to stress that the moment depends on the parameters of the distribution.
$\mu_z$	$z^{\text{th}}$ central moment (moment about the mean) of a distribution.
$A$	The adjacency matrix of an undirected graph.
$A_{ij}$	Coefficient of the adjacency matrix.
$N$	A matrix whose entries $(N_{ij}, N_{ji})$ are sampled from a bivariate normal distribution.
$U$	A matrix whose entries are sampled from a uniform distribution.
$M$	Matrix obtained by multiplying the elements of $A$ and $N$ (or $U$ ).
$\text{Tr}(M)$	Trace of the matrix $M$ .
$M^z$	Matrix $M$ raised to the $z^{\text{th}}$ power.
$k$	The average degree of the nodes in a network described by $A$ .
$s$	Size of the network.
$\lambda_i$	$i^{\text{th}}$ eigenvalue of a matrix.
$i$	$\sqrt{-1}$ .
$a$	Horizontal radius of a superellipse.
$b$	Vertical radius of a superellipse.
$r$	$(a + b)/2$ .
$n$	Shape parameter of a superellipse.
$\Gamma(\cdot)$	Gamma function.

## Superelliptical distributions

### Matrices and Graphs.

We analyze matrices  $M$  of size  $s \times s$  that are obtained by multiplying the elements of two matrices:  $M_{ij} = A_{ij}N_{ij}$ .  $A$  is the adjacency matrix of an undirected, simple graph without self-loops, generated by the configuration model[24, 14] (for a particular degree distribution). The nodes in the graph have average degree  $k$ . We consider the case of integer  $k$ , with  $k > 1$ , so that the graph is almost surely connected, and  $k \leq (s - 1)$ , as the graph does not contain self-loops. Thus, the adjacency matrix contains exactly  $sk$  nonzero coefficients.  $N$  is a matrix whose elements  $(N_{ij}, N_{ji})$  are sampled from a normal bivariate distribution  $\mathcal{N}(\boldsymbol{\mu}, \boldsymbol{\Sigma})$ , with

$$\boldsymbol{\mu} = \begin{bmatrix} 0 \\ 0 \end{bmatrix} \quad (\text{S1})$$

and

$$\boldsymbol{\Sigma} = \begin{bmatrix} \frac{1}{k} & \frac{\rho}{k} \\ \frac{\rho}{k} & \frac{1}{k} \end{bmatrix} \quad (\text{S2})$$

Clearly,  $\mathbb{E}[M_{ij}] = 0$ , and  $\text{Var}[M_{ij}] = \mathbb{E}[M_{ij}^2] = 1/s$ . For  $k \rightarrow \infty$ , each value of the Pearson's correlation coefficient  $\rho$  determines which of the following well-known laws describes the distribution of the eigenvalues



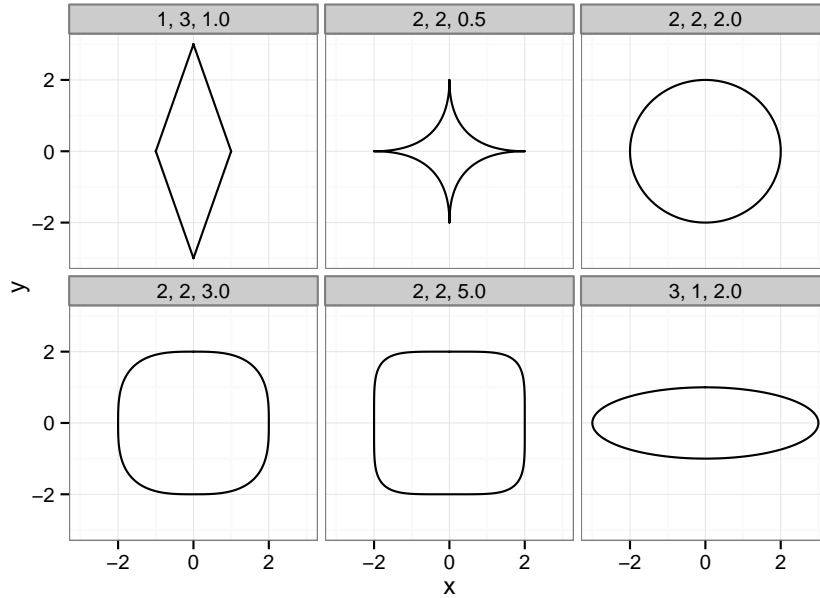


Figure S1: Shapes of  $|x|^n/a^n + |y|^n/b^n = 1$ , for different values of  $a$ ,  $b$  and  $n$  (panel titles).

of  $M$ :

$\rho$	Law
1	Wigner's semicircle law[9]
0	Girko's circular law[17, 10, 18]
$-1 < \rho < 1$	Elliptical law[19, 20, 21]

We want to study the case in which  $k \ll s$ , and the structure of the graph  $A$  is generated using different degree distributions. In particular, we analyze degree distributions obtained from  $k$ -regular random graphs, Erdős-Rényi random graphs[26], and Power-law (scale-free) graphs[13]. All graphs were generated using the `igraph` library[27] for the statistical software R[28]. For Power-law graphs, undirected networks were obtained using the routine `static.power.law.game` with a power-law exponent of 2.5.

To obtain higher precision, we transform the nonzero coefficients of the matrix  $M$  to ensure that  $\overline{M}_{ij} = 0$  and  $\overline{M}^2_{ij} = 1/s$ .

## Superellipses.

As we will show, the eigenvalues of matrices with complex network structure are described by superellipses. A superellipse is defined by the equation:

$$\frac{|x|^n}{a^n} + \frac{|y|^n}{b^n} = 1 \quad (\text{S3})$$

For  $n = 2$  we recover the equation describing an ellipse (a circle when  $a = b$ ). The area of a superellipse is  $4ab\Gamma(1 + 1/n)^2\Gamma(1 + 2/n)^{-1}$ . Superellipses can take dramatically different shapes depending on the parameter values (Figure S1).

## Moments of the eigenvalue distribution.

A superellipse is defined by three parameters:  $a$ ,  $b$  and  $n$ . When deriving the parameters, we will use some well-known identities relating the traces of the powers of a matrix to its eigenvalue distribution.

In particular, we will construct equations whose left-hand-side is obtained integrating the probability density function of the eigenvalue distribution, and the right-hand-side by exploiting identities based on the traces of the powers of a matrix.

We write  $\mu'_z$  for the  $z^{\text{th}}$  raw moment (moment about the origin) of the eigenvalue distribution, and  $\mu_z$  for the corresponding central moment (moment about the mean). For any matrix with zero on the diagonal (and hence  $\bar{\lambda} = 0$ ), the raw and central moment are the same:

$$\mu'_z = \mu_z = \frac{1}{s} \sum_{j=1}^s \lambda_j^z = \frac{\text{Tr}(M^z)}{s} \quad (\text{S4})$$

Because we are dealing with real matrices, all eigenvalues are either real or complex conjugates. It follows that all the moments  $\mu'_z$  are real. Moreover, this greatly simplifies the integrals for the moments. We write  $\lambda_j = x_j + iy_j$ , where  $i = \sqrt{-1}$ . The integral for the second moment is:

$$\mu'_2 = \mu_2 = \int \lambda^2 P(\lambda) d\lambda = \iint (x + iy)^2 P(x, y) dx dy = \iint (x^2 - y^2 + 2ixy) P(x, y) dx dy \quad (\text{S5})$$

where  $P(\cdot)$  is the probability density function. Because the complex eigenvalues are paired, if  $x + iy$  is an eigenvalue, so is  $x - iy$ . Hence, the imaginary part vanishes from the integral, leaving

$$\mu'_2 = \mu_2 = \iint (x^2 - y^2) P(x, y) dx dy \quad (\text{S6})$$

Similarly, we can write

$$\mu'_4 = \mu_4 = \iint (x^4 + y^4 - 6x^2y^2) P(x, y) dx dy \quad (\text{S7})$$

## Semi-superelliptical distribution.

As in the main text, we start by setting  $\rho = 1$ , so that  $M$  is symmetric (Hermitian). In this case, all eigenvalues are real, simplifying the problem. Whenever  $\rho = -1$ ,  $M$  is skew-symmetric, and all eigenvalues are imaginary.

For  $\rho = 1$  and  $k \rightarrow \infty$ , the eigenvalue distribution is described by Wigner's semicircle law:

$$\text{Pr}(\lambda = x) = P(x) = \frac{2\sqrt{(2r)^2 - x^2}}{(2r)^2\pi} \quad (\text{S8})$$

where we write the radius as  $a = 2r$  to make the derivation consistent with the asymmetric case below. The distribution of the eigenvalues has mean 0, and variance:

$$\mu_2(r) = \int_{-2r}^{2r} x^2 P(x) dx = r^2 \quad (\text{S9})$$

Because, for these matrices

$$\mu_2(r) = \frac{\text{Tr}(M^2)}{s} = \mathbb{E}[M_{ij}M_{ji}] = \mathbb{E}[M_{ij}^2] = 1 \quad (\text{S10})$$

then necessarily  $r = 1$ .

We want to extend Wigner's semicircle law to the case of matrices with complex network structure. We hypothesize that in this case, the density of the eigenvalues follows a semi-superellipse:

$$\text{Pr}(\lambda = x) = P(x) = \frac{2\sqrt{(2r)^n - x^n}}{4(2r)^2\Gamma(1 + 1/n)^2\Gamma(1 + 2/n)^{-1}} \quad (\text{S11})$$

Because we have two parameters,  $r$  and  $n$ , we need to compute two moments. The first two nonzero moments for this distribution are  $\mu_2(r, n)$  and  $\mu_4(r, n)$ .

$$\mu_2(r, n) = \int_{-2r}^{2r} x^2 P(x) dx = r^2 \frac{2\Gamma(\frac{2}{n}) \Gamma(\frac{3}{n})}{\Gamma(\frac{1}{n}) \Gamma(\frac{4}{n})} \quad (\text{S12})$$

Given that also in this case we have  $\mu_2(r, n) = 1$ , we can solve for the positive  $r$ :

$$r = \sqrt{\frac{\Gamma(\frac{1}{n}) \Gamma(\frac{4}{n})}{2\Gamma(\frac{2}{n}) \Gamma(\frac{3}{n})}} \quad (\text{S13})$$

Integrating to obtain  $\mu_4(r, n)$ :

$$\mu_4(r, n) = \int_{-2r}^{2r} x^4 P(x) dx = \frac{8r^4 \Gamma(\frac{1}{n}) \Gamma(1 + \frac{2}{n}) \Gamma(1 + \frac{5}{n})}{15\Gamma(1 + \frac{1}{n})^2 \Gamma(\frac{6}{n})} \quad (\text{S14})$$

and substituting the value of  $r$ :

$$\mu_4(n) = \frac{2\Gamma(\frac{1}{n})^3 \Gamma(\frac{4}{n})^2 \Gamma(1 + \frac{2}{n}) \Gamma(1 + \frac{5}{n})}{15\Gamma(1 + \frac{1}{n})^2 \Gamma(\frac{2}{n})^2 \Gamma(\frac{3}{n})^2 \Gamma(\frac{6}{n})} \quad (\text{S15})$$

Hence, knowing the value of  $\mu_4(n) = \text{Tr}(M^4)/s$ , we can numerically solve the equation above for  $n$ , and recover  $a = 2r$  from  $n$  using Eq. (S13).

### **$k$ -regular graphs: superelliptical distribution.**

We now derive the superelliptical distribution for eigenvalues that are uniformly distributed in a superellipse. Our simulations show that this is the case for matrices whose underlying structure is a  $k$ -regular random graph. For those generated using Erdős-Rényi random graphs, the distribution slightly departs from uniformity, and for those built using Power-law graphs, it departs severely. Hence, only for the case of  $k$ -regular graphs do we expect the superelliptical uniform distribution to hold.

We make only one assumption in order to derive the values of  $n$  and  $r$ . We assume that  $a + b = 2r$  irrespective of  $\rho$ . This assumption is strongly supported by numerical simulations for the case of  $k$ -regular random graphs (the only case in which we believe the following results to hold). When  $a + b = 2r$  for any  $\rho$ , the semi-superelliptical distribution derived above is recovered for  $\rho = 1$ . As such, the value of  $r$  is that in Eq. (S13).

As we did above, we first compute the moments using the eigenvalue distribution, and then derive the right-hand-sides of the equations using traces.

The probability density function for eigenvalues uniformly distributed in the superellipse  $|x|^n/a^n + |y|^n/b^n \leq 1$  is:

$$P(x, y) = \frac{1}{4ab\Gamma(1 + 1/n)^2 \Gamma(1 + 2/n)^{-1}} \quad (\text{S16})$$

Integrating  $(x^2 - y^2)$  we obtain  $\mu_2(a, b, n)$ :

$$\mu_2(a, b, n) = \int_{-a}^a \int_{-\frac{b}{a} \sqrt[n]{a^n - |x|^n}}^{\frac{b}{a} \sqrt[n]{a^n - |x|^n}} (x^2 - y^2) P(x, y) dy dx = \frac{(a - b)(a + b) \Gamma(\frac{2}{n}) \Gamma(\frac{3}{n})}{2\Gamma(\frac{1}{n}) \Gamma(\frac{4}{n})} \quad (\text{S17})$$

Because  $\mu_2(a, b, n) = \mathbb{E}[M_{ij}M_{ji}] = \rho$ , we can set  $b = 2r - a$  and solve for  $a$ :

$$a = r + \frac{\rho \Gamma(\frac{1}{n}) \Gamma(\frac{4}{n})}{2r \Gamma(\frac{2}{n}) \Gamma(\frac{3}{n})} = r(1 + \rho) \quad (\text{S18})$$

Similarly,  $b = r(1 - \rho)$ , consistently with the fact that, when  $k \rightarrow \infty$ , then  $a = 1 + \rho$  and  $b = 1 - \rho$  (elliptical law [19, 20, 21]).

We then move to the fourth moment:

$$\begin{aligned}
\mu_4(a, b, n) &= \int_{-a}^a \int_{-\frac{b}{a}\sqrt[n]{a^n-|x|^n}}^{\frac{b}{a}\sqrt[n]{a^n-|x|^n}} (x^4 + y^4 - 6x^2y^2)P(x, y)dydx = \\
&= \frac{a^4\Gamma(\frac{1}{n})\Gamma(1+\frac{2}{n})\Gamma(1+\frac{5}{n})}{30\Gamma(1+\frac{1}{n})^2\Gamma(\frac{6}{n})} + \\
&\quad \frac{b^4\Gamma(1+\frac{2}{n})\Gamma(1+\frac{5}{n})}{5\Gamma(1+\frac{1}{n})\Gamma(1+\frac{6}{n})} - \\
&\quad \frac{a^2b^22^{1-\frac{4}{n}}\Gamma(\frac{1}{2}+\frac{1}{n})\Gamma(\frac{3}{n})}{30\Gamma(1+\frac{1}{n})^2\Gamma(\frac{6}{n})}
\end{aligned} \tag{S19}$$

Substituting  $a = r(1 + \rho)$ ,  $b = r(1 - \rho)$  and replacing  $r$  with the value in Eq. (S13) greatly simplifies the expression:

$$\mu_4(n, \rho) = \frac{2^{\frac{4}{n}-2}\Gamma(\frac{1}{2}+\frac{2}{n})\Gamma(\frac{4}{n})\left(\frac{(\rho^4+6\rho^2+1)\Gamma(\frac{1}{n})\Gamma(\frac{5}{n})}{\Gamma(\frac{3}{n})^2} - 3(1-\rho^2)^2\right)}{3\sqrt{\pi}\Gamma(\frac{6}{n})} \tag{S20}$$

Knowing  $\rho$  and  $\text{Tr}(M^4)$ , we solve this equation numerically to obtain  $n$ , use Eq. (S13) to obtain  $r$ , and, finally, use  $r$  and  $\rho$  to compute  $a$  and  $b$ .

## Computing expected traces.

Above, we computed the values of  $n$ ,  $a$  and  $b$  using the actual, observed traces of  $M^2$  and  $M^4$ :  $\mu_2 = \text{Tr}(M^2)/s$  and  $\mu_4 = \text{Tr}(M^4)/s$ . Alternatively, one can compute the expectations for the traces when the distribution of the coefficients is known and one can count certain structures in the graph. Clearly  $\mathbb{E}[\text{Tr}(M^2)/s] = \rho$ . The computation of  $\mathbb{E}[\text{Tr}(M^4)/s]$  is detailed below for the case of symmetric and asymmetric matrices. Because the results are particularly simple for matrices with  $k$ -regular graph structure, we explore the effect of the average degree on the parameters of the superellipses in this case.

**Symmetric matrices.** Only four possible network structures contribute to the fourth power of  $M$  in the graphs analyzed here. In fact, the diagonal element  $M_{jj}^4$  is composed of the sum of the closed paths involving four links that start and end at node  $j$ . There are four possibilities (Table S2, all indices are taken to be different -  $j \neq l \neq n \neq m$ ):

- T1)  $M_{jl}M_{lj}M_{jl}M_{lj}$ , i.e., the same undirected link tread twice. For symmetric matrices, we can write  $M_{jl}^4$ .
- T2)  $M_{jl}M_{lj}M_{jm}M_{mj}$ , i.e., a path where we move from  $j$  to  $l$ , come back and then move to  $m$  and come back. For symmetric matrices, we can write  $M_{jl}^2M_{jm}^2$ .
- T3)  $M_{jl}M_{lm}M_{ml}M_{lj}$ , i.e., a path where we move from  $j$  to  $l$ , from  $l$  to  $m$  and then go back to  $l$  and finally to  $j$ . For symmetric matrices, we can write  $M_{jl}^2M_{lm}^2$ .
- T4)  $M_{jl}M_{lm}M_{mn}M_{nj}$ , i.e., a four-link directed cycle.

For each graph, we can count how many ways there are to obtain each structure:

- T1) There is an occurrence of T1 for each connection in the graph. Thus, the total number of structures of this kind is  $sk$ .
- T2) For a node of degree  $k_j$ , there are  $\binom{k_j}{2}$  ways of choosing the two partners. However, for each choice of partners ( $l$  and  $m$ ) we have two possibilities: visit  $l$  first, and visit  $m$  first. Hence, the number of structures is:  $2\sum_{j=1}^s \binom{k_j}{2}$ .
- T3) For each edge connecting  $j$  to  $l$ , we have  $k_l - 1$  ways of choosing the third partner. Thus, the number of structures is  $\sum_{j=1}^s \sum_{l=1}^s A_{jl}(k_l - 1)$ .

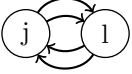
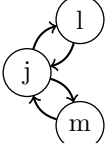
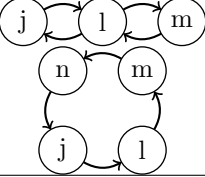
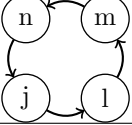
Type	Graph	Coefficients	Number of Occurrences	Expectation
T1		$M_{jl}M_{lj}M_{jl}M_{lj} = M_{jl}^4$	$sk$	$\frac{3}{k^2}$
T2		$M_{jl}M_{lj}M_{jm}M_{mj} = M_{jl}^2M_{jm}^2$	$2 \sum_{j=1}^s \binom{k_j}{2}$	$\frac{1}{k^2}$
T3		$M_{jl}M_{lm}M_{ml}M_{lj} = M_{jl}^2M_{lm}^2$	$\sum_{j=1}^s \sum_{l=1}^s A_{jl}(k_l - 1)$	$\frac{1}{k^2}$
T4		$M_{jl}M_{lm}M_{mn}M_{nj}$	Depends on graph	0

Table S1: The structures contributing to  $\text{Tr}(M^4)$ . For each structure, we report the form of the coefficients, the number of occurrences in a graph, and the expected value when the coefficients are taken from a bivariate normal distribution with correlation  $\rho = 1$ .

T4) The number of four-cycles in the graph cannot be expressed as a simple function of the degrees of the nodes.

Finally, we need to compute the expectation for their values. For the normal bivariate distribution described above, we have:

T1)  $\mathbb{E}[M_{jl}M_{lj}M_{jl}M_{lj}] = \mathbb{E}[M_{jl}^4] = \frac{3}{k^2}$ , as the fourth central moment of a normal distribution  $\mathcal{N}(0, \sigma^2)$  is simply  $3\sigma^2$ .

T2)  $\mathbb{E}[M_{jl}M_{lj}M_{jm}M_{mj}] = \mathbb{E}[M_{jl}^2M_{jm}^2] = \frac{1}{k^2}$  (the product of the two variances).

T3)  $\mathbb{E}[M_{jl}M_{lm}M_{ml}M_{lj}] = \mathbb{E}[M_{jl}^2M_{lm}^2] = \frac{1}{k^2}$ .

T4)  $\mathbb{E}[M_{jl}M_{lm}M_{mn}M_{nj}] = 0$ , as the expectation of the product is simply the product of the expectations – all the coefficients are independent.

Given that  $\mathbb{E}[T4] = 0$ , summing ( $\#T1 \cdot \mathbb{E}[T1] + \#T2 \cdot \mathbb{E}[T2] + \#T3 \cdot \mathbb{E}[T3]$ ) we obtain  $\mathbb{E}[\text{Tr}(M^4)]$ . Dividing by  $s$ , we obtain  $\mathbb{E}[\text{Tr}(M^4)/s] = \mu_4(n)$ . The calculation is especially simple for a  $k$ -regular graph, in which we can count the number of T2 and T3 structures very easily. For this type of graph,  $\mathbb{E}[\text{Tr}(M^4)/s] = 2 + \frac{1}{k}$ .

**Asymmetric matrices.** As in the case of symmetric matrices, the expectation  $\mathbb{E}[\text{Tr}(M^4)/s]$  can be obtained counting the structures T1, T2 and T3 in the graph. However, we need to re-compute the expectations for the structures for arbitrary  $\rho$  (Table S3). For a  $k$ -regular random graph, we have  $\mathbb{E}[\text{Tr}(M^4)/s] = 2\rho^2 + \frac{1}{k}$ .

**$k$ -regular graphs.** As shown in the two sections above, for a matrix  $M$  with  $k$ -regular graph structure, we have that  $\mathbb{E}[\text{Tr}(M^2)/s] = \rho$ , and  $\mathbb{E}[\text{Tr}(M^4)/s] = 2\rho^2 + \frac{1}{k}$ . As such, we can easily find the expected  $n$  and  $r$  for any value of  $\rho$  and  $k$ . We find that, when increasing  $k$ ,  $r$  converges to 1 quite rapidly, while the value of  $n$  converges to 2 more slowly. Because the value of  $r$  depends only on  $n$ , and the value of  $n$  depends on the average degree  $k$  and on  $\rho^2$ , without loss of generality we can assume  $\rho$  to be positive. The results show that a strong correlation (large  $\rho$ ) speeds up the convergence of both  $r$  and  $n$  (Figure S2).

## Supplementary Results.

**Normal bivariate distribution, negative correlation.** In the main text, we drew the eigenvalue distributions for asymmetric matrices with complex network structure when  $\mathbb{E}[\rho] = 0$  (Figure 2) and  $\mathbb{E}[\rho] = 0.5$  (Figure 3). In Figure S3, we show the case of  $\mathbb{E}[\rho] = -0.5$ .

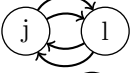
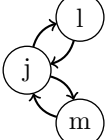

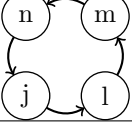
Type	Graph	Coefficients	Number of Occurrences	Expectation
T1		$M_{jl}M_{lj}M_{jl}M_{lj} = M_{jl}^2M_{lj}^2$	$sk$	$\frac{1+2\rho^2}{k^2}$
T2		$M_{jl}M_{lj}M_{jm}M_{mj}$	$2 \sum_{j=1}^s \binom{k_j}{2}$	$\frac{\rho^2}{k^2}$
T3		$M_{jl}M_{lm}M_{ml}M_{lj}$	$\sum_{j=1}^s \sum_{l=1}^s A_{jl}(k_l - 1)$	$\frac{\rho^2}{k^2}$
T4		$M_{jl}M_{lm}M_{mn}M_{nj}$	Depends on graph	0

Table S2: *The structures contributing to  $\text{Tr}(M^4)$ . For each structure, we report the form of the coefficients, the number of occurrences in a graph, and the expected value when the coefficients are taken from a bivariate normal distribution with correlation  $\rho$ .*

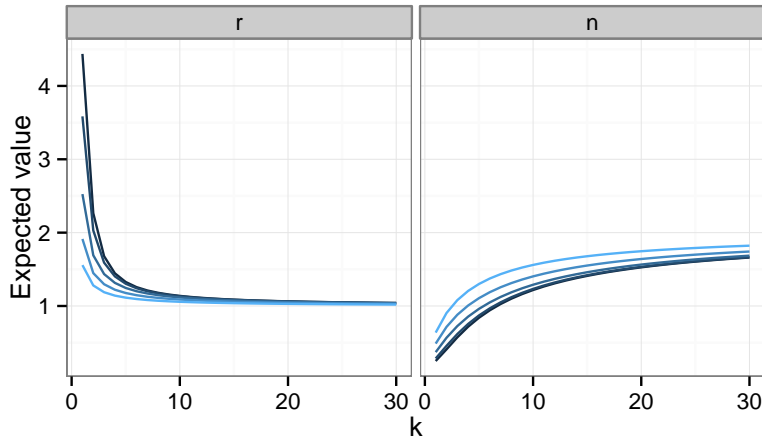


Figure S2: *Expected  $r$  and  $n$  for matrices whose underlying structure is a  $k$ -regular graph of degree  $k$  ( $x$ -axis). Colors represent the value of  $\rho$  (from 0 – darker color, to 1).*

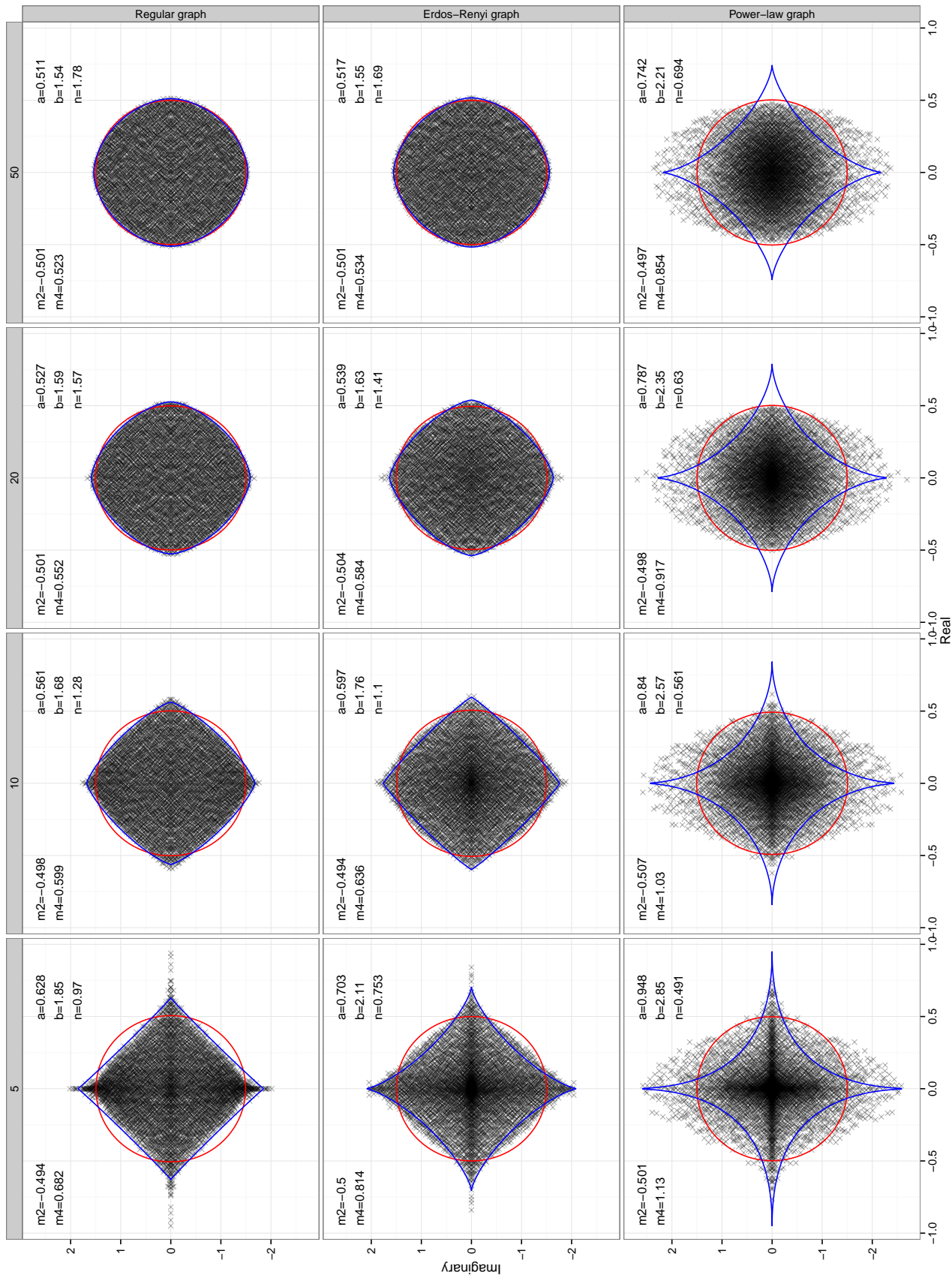


Figure S3: As main text Figure 2 and Figure 3, but with negative correlation:  $\mathbb{E}[\rho] = -0.5$ .

**Uniform distribution.** Girko’s circular law has been recently shown to be universal, i.e., the law holds given very mild conditions on the distribution of the coefficients in the matrix[18]. Hence, it is interesting to test whether choosing different distributions for the coefficients in the matrix significantly alters the superelliptical distribution. As with Girko’s circular law, we find that our results hold for different distributions.

For example, take symmetric matrices whose coefficients are sampled from a uniform distribution. We set  $M_{ij} = M_{ji} = A_{ij}U_{ij}$ , where  $U$  is a symmetric matrix whose coefficients come from  $\mathcal{U}(-\sqrt{3/k}, \sqrt{3/k})$ , so that  $\mathbb{E}[M_{ij}] = 0$ , and  $\text{Var}[M_{ij}] = \mathbb{E}[M_{ij}^2] = 1/s$ . The eigenvalue density follows the semi-superelliptical distribution, as shown in Figure S4.

Similarly, make the coefficients in  $U$  independent identically distributed: then matrices whose underlying structure are  $k$ -regular graphs follow the superelliptical distribution (Figure S5).

## Approximating the largest eigenvalue of adjacency matrices

In the analysis above, we assumed the mean of the coefficients of  $M$  to be 0. The problem is more complicated when this is not the case. However, many applications deal with non-negative matrices (i.e., whose entries are  $\geq 0$ ), and therefore it is important to extend the methods above to encompass such cases.

In the following paragraphs, we deal with adjacency matrices of undirected graphs with complex network structure. This case is particularly well-studied, given the potential for applications, and many bounds on the largest eigenvalue (spectral radius) have been proposed (for a brief survey, see Das & Kumar[29]). One of the simplest and most beautiful approximations for the largest eigenvalue is that proposed by Chung *et al.*[15]:  $\lambda_1 \approx \bar{k}^2/\bar{k}$  (the average of the squared degrees divided by the average degree). This approximation—which was also derived using a completely different approach by Nadakuditi & Newman[16]—is expected to hold whenever the minimum degree is large enough compared to the average degree:  $\min(k_i) \gg \sqrt{\bar{k}} \log^3 s$ .

The spectrum of the adjacency matrix of a complex network generally departs severely from Wigner’s semicircle[12]. Moreover, although the “bulk” of the eigenvalues falls in a well-defined region, the largest eigenvalue,  $\lambda_1$ —and, possibly, other large eigenvalues—is not localized in this region.

Here we present a novel method to estimate the value of  $\lambda_1$  obtained assuming that all the other eigenvalues fall in a symmetric distribution, such as a semi-superellipse. This seems to be the case for adjacency matrices of random graphs with arbitrary degree distributions built using the configuration model (Figure S6).

We consider the adjacency matrix  $A$ , describing a simple, undirected graph without self-loops. In this matrix, the diagonal is 0, and therefore the mean of the eigenvalues is zero. We can write:

$$\text{Tr}(A) = 0 = \sum_{i=1}^s \lambda_i = \lambda_1 + \sum_{i=2}^s \lambda_i \quad (\text{S21})$$

where  $\lambda_1$  is the largest eigenvalue (spectral radius). We want to describe the distribution of the non-dominant eigenvalues  $\lambda_2, \dots, \lambda_s$ . In general, we can write:

$$\text{Tr}(A^j) = \sum_{i=1}^s \lambda_i^j = s\mu'_j \quad (\text{S22})$$

That is, the trace of the  $j^{\text{th}}$  power of  $M$  is equal to the size  $s$  times the  $j^{\text{th}}$  raw moment of the eigenvalue distribution. When we consider  $\lambda_1$  separately, we have:

$$\text{Tr}(A^j) = s\mu'_j = (s-1)\tilde{\mu}'_j + \lambda_1^j \quad (\text{S23})$$

where with  $\tilde{\mu}'_j$  we indicate the  $j^{\text{th}}$  raw moment of the distribution of the eigenvalues when we exclude the dominant one. Because the trace of the matrix is zero, we have:

$$\text{Tr}(A) = 0 = (s-1)\tilde{\mu}'_1 + \lambda_1 \rightarrow \tilde{\mu}'_1 = -\frac{\lambda_1}{s-1} \quad (\text{S24})$$

The trace of  $A^2$  is simply the number of connections:

$$\text{Tr}(A^2) = sk = (s-1)\tilde{\mu}'_2 + \lambda_1^2 \rightarrow \tilde{\mu}'_2 = \frac{sk - \lambda_1^2}{s-1} \quad (\text{S25})$$



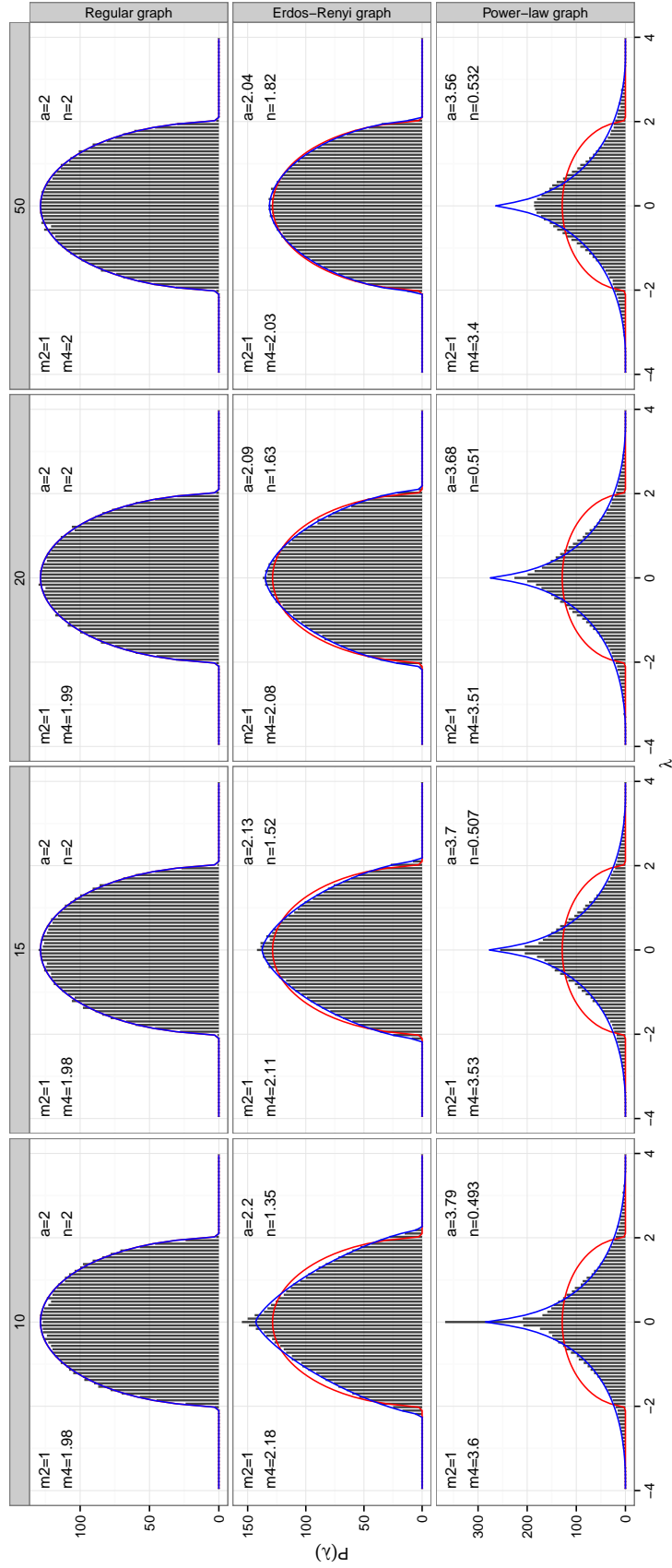


Figure S4: As main text Figure 1, but with entries  $M_{ij} = M_{ji} = A_{ij}U_{ij}$ , where  $U$  is a symmetric matrix with uniformly distributed coefficients (see text).

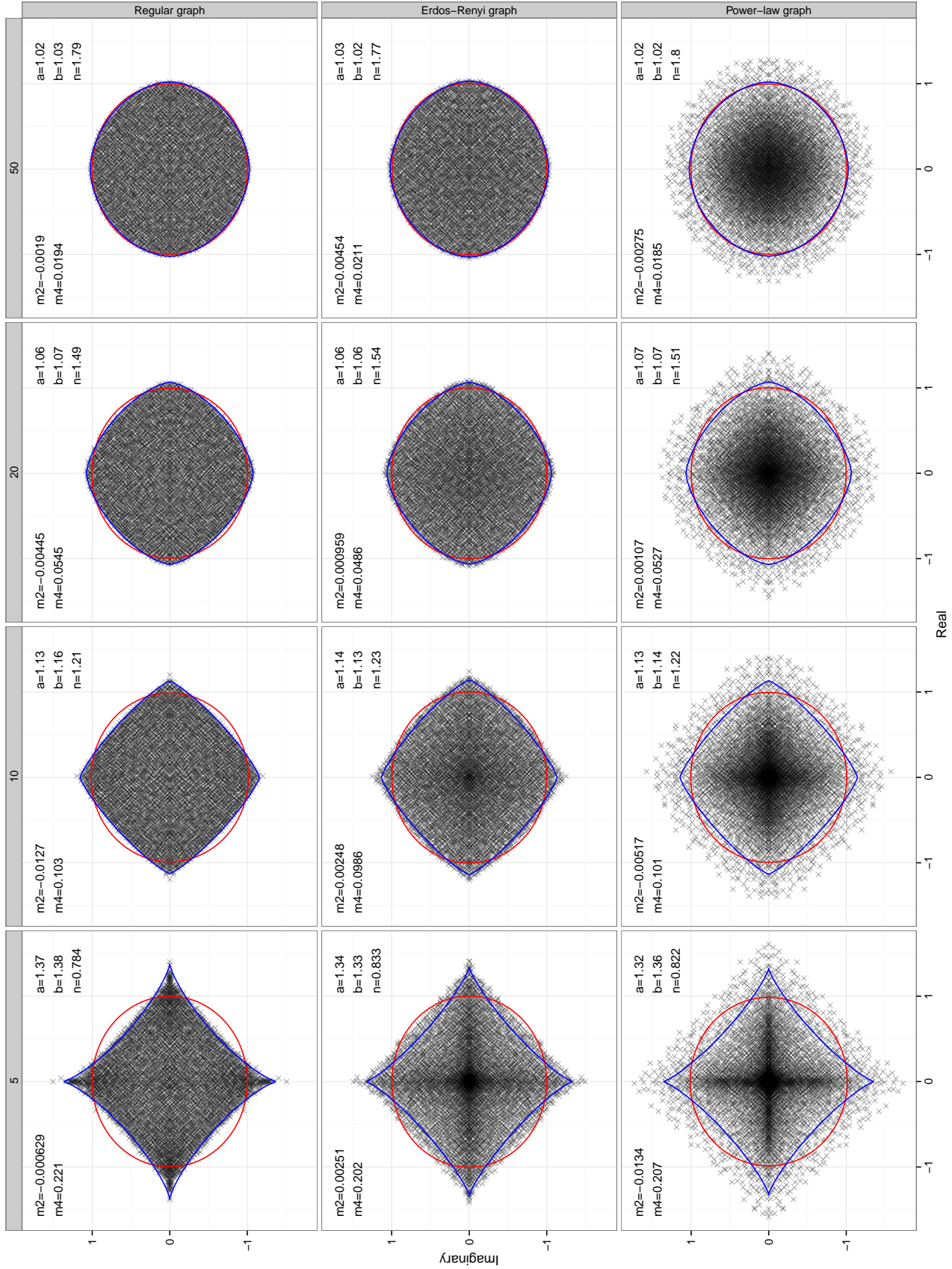


Figure S5: As main text Figure 2, but with entries  $M_{ij} = A_{ij}U_{ij}$ , where  $U$  is a matrix whose coefficients are uniformly distributed.

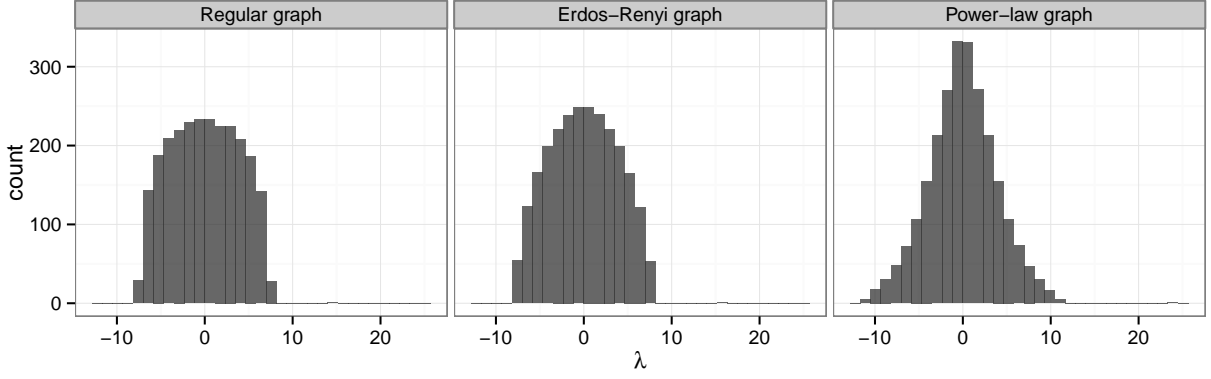


Figure S6: Spectra of adjacency matrices of size 2500 built using the configuration model with average degree  $k = 15$ , and degree distributions specified by different models. In all cases, the spectrum can be approximated by a semi-superellipse containing all the eigenvalues but the dominant one, plus  $\lambda_1$  itself.

In general, the  $j^{\text{th}}$  raw moment is:

$$\tilde{\mu}'_j = \frac{\text{Tr}(A^j) - \lambda_1^j}{s - 1} \quad (\text{S26})$$

If the distribution of all the eigenvalues but  $\lambda_1$  is approximately symmetric, then the odd central moments  $\tilde{\mu}_{2j+1} \approx 0$ . We can exploit this fact to approximate the value of  $\lambda_1$ . First, we need the following formulas relating raw and central moments:

$$\begin{aligned} \mu'_3 &= \mu_3 + 3\mu'_1\mu'_2 - 2(\mu'_1)^3 \\ \mu'_5 &= \mu_5 + 5\mu'_1\mu'_4 - 10(\mu'_1)^2\mu'_3 + 10(\mu'_1)^3\mu'_2 - 4(\mu'_1)^5 \end{aligned} \quad (\text{S27})$$

Then, we can for example, choose  $\tilde{\mu}_3 \approx 0$ . In this case,

$$\text{Tr}(A^3) = (s - 1)\tilde{\mu}'_3 + \lambda_1^3 \approx (s - 1)(3\tilde{\mu}'_1\tilde{\mu}'_2 - 2(\tilde{\mu}'_1)^3) + \lambda_1^3 \quad (\text{S28})$$

Substituting the values for  $\tilde{\mu}'_1$  and  $\tilde{\mu}'_2$ , we obtain:

$$\lambda_1^3 \frac{s(s+1)}{(s-1)^2} - \lambda_1 \frac{3ks}{s-1} \approx \text{Tr}(A^3) \quad (\text{S29})$$

which, assuming equality, we can solve numerically, or analytically (taking the only real value):

$$\lambda_1 \approx \frac{-\sqrt[3]{2} \left( s^2 (s^2 - 1) \left( \sqrt{(s^2 - 1)((s^2 - 1)\text{Tr}(A^3)^2 - 4k^3s^2)} + s^2(-\text{Tr}(A^3)) + \text{Tr}(A^3) \right) \right)^{2/3} - 2ks^2(s^2 - 1)}{2^{2/3}s(s+1)\sqrt[3]{s^2(s^2 - 1) \left( \sqrt{(s^2 - 1)((s^2 - 1)\text{Tr}(A^3)^2 - 4k^3s^2)} + s^2(-\text{Tr}(A^3)) + \text{Tr}(A^3) \right)}} \quad (\text{S30})$$

Similarly, we can choose to zero a higher moment. For example, if  $\tilde{\mu}_5 \approx 0$ , we have:

$$\text{Tr}(A^5) = (s - 1)\tilde{\mu}'_5 + \lambda_1^5 \approx (s - 1) \left( 5\tilde{\mu}'_1\tilde{\mu}'_4 - 10(\tilde{\mu}'_1)^2\tilde{\mu}'_3 + 10(\tilde{\mu}'_1)^3\tilde{\mu}'_2 - 4(\tilde{\mu}'_1)^5 \right) + \lambda_1^5 \quad (\text{S31})$$

which yields

$$\lambda_1^5 \frac{s(s+1)(s^2+1)}{(s-1)^4} - \lambda_1^3 \frac{10sk}{(s-1)^3} - \lambda_1^2 \frac{10\text{Tr}(A^3)}{(s-1)^2} - \lambda_1 \frac{5\text{Tr}(A^4)}{(s-1)} \approx \text{Tr}(A^5) \quad (\text{S32})$$

Assuming equality, one can solve the equation numerically. Clearly, one can derive an approximation assuming any of the odd central moments  $\tilde{\mu}_{2j+1}$  to be zero.

## Beyond the configuration model: the spectra of real networks

In the previous sections, we dealt with matrices whose underlying structure was built using the configuration model. That is, the networks contain no special structure, besides the imposition of a degree distribution. They are, in a way, “random networks”. Here we explore the sensitivity of our results to the use of networks that depart considerably from this assumption. In fact, the ultimate test for any of these methods is to be able to deal with real-world networks.

We repeat the analysis above using three different data sets: i) networks built according to the Watts-Strogatz model[30]; ii) networks built with the Barabási-Albert model[13]; and, iii) A set of four networks of biological interest, describing a) the structure of the contact network in an high school[31], b) the neural network of the worm *C. elegans*[32, 30], c) the metabolic network of *C. elegans*[33] and, d) the food web structure of the Weddell Sea ecosystem[34]. For simplicity, all the networks are taken to be undirected.

For the networks built using the Watts-Strogatz model, we set  $s = 5000$ , and arranged the nodes in a one-dimensional lattice without boundaries. Each node is connected to the  $k/2$  nodes on its left and to its right, forming a regular, one-dimensional lattice. Links are then rewired with probability 0.05. This can be accomplished calling the routine `watts.strogatz.game(1, 5000, k/2, 0.05)` in `igraph`.

For the networks built using the Barabási-Albert model, we built networks of size  $s = 5000$  using preferential attachment with exponent 1, where each node introduced in the network attaches to  $k/2$  nodes (if possible). The corresponding routine in `igraph` is `barabasi.game(5000, power = 1, m = k/2, directed = FALSE)`.

**Symmetric matrices.** We used the empirical networks and those built using the two models above to construct the symmetric matrices  $M$  (i.e.,  $M_{ij} = A_{ij}N_{ij}$ , where  $N$  is symmetric). The semi-superelliptical distribution captures the eigenvalues of  $M$  (Figures S7 and S8).

**Asymmetric matrices.** We repeated the exercise using asymmetric matrices, and found, that the superelliptical distribution describes the eigenvalues quite poorly—as expected—, with the exception of the Watts-Strogatz model and the High school contact network (Figures S9 and S10).

**Approximating  $\lambda_1$ .** Finally, we constructed a hundred  $1000 \times 1000$  adjacency matrices for each choice of  $k$  using the two models and attempted to approximate  $\lambda_1$ . For the Watts-Strogatz model, the approximation of Chung *et al.* is clearly superior, while for the Barabási-Albert model and the empirical networks the new approximations introduced here produce better results (Figure S11 and S12).

## Code

Code performing the analysis described here is freely available for download in the public repository:  
<https://bitbucket.org/AllesinaLab/superellipses>.

## Acknowledgments

Research supported by NSF DEB #1148867. We thank J. Grilli and P. Staniczenko for comments.

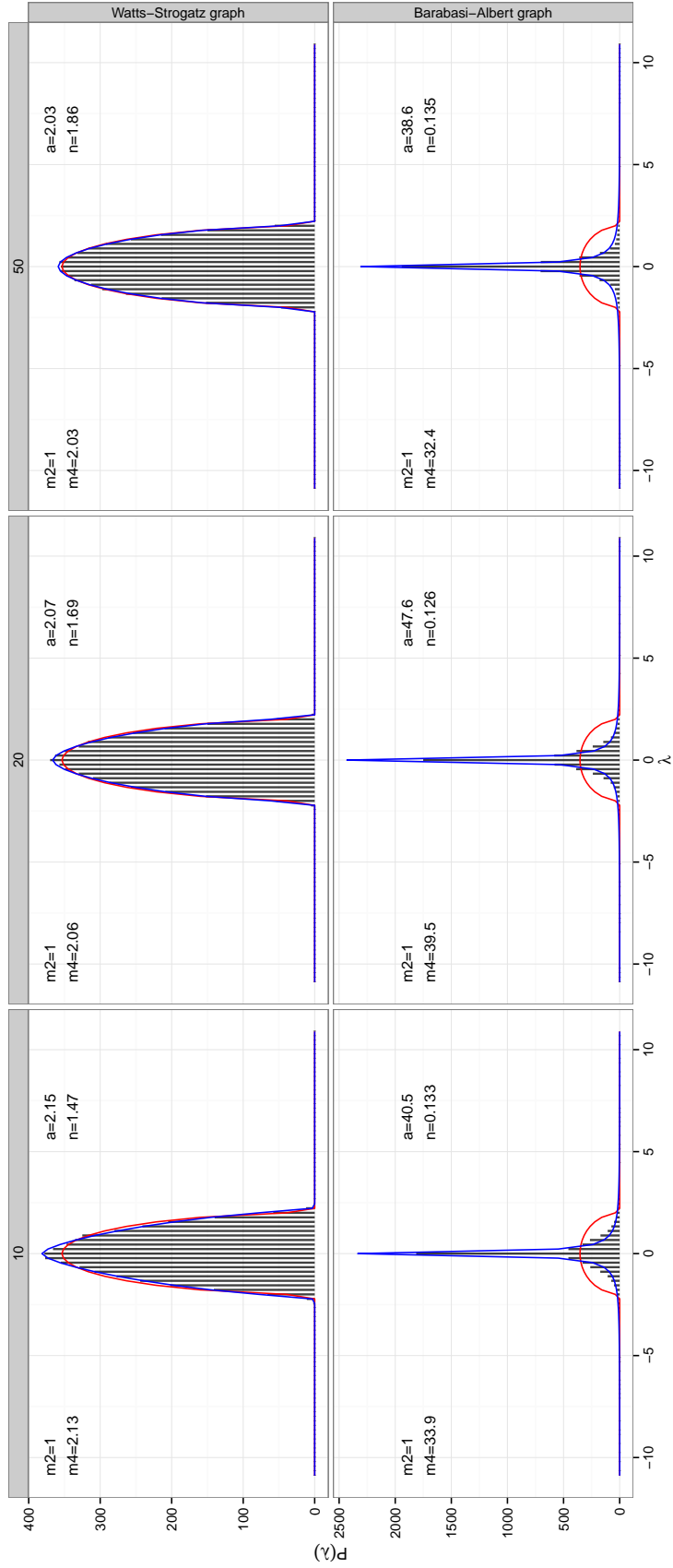


Figure S7: As main text Figure 1, but using different models to construct the networks.

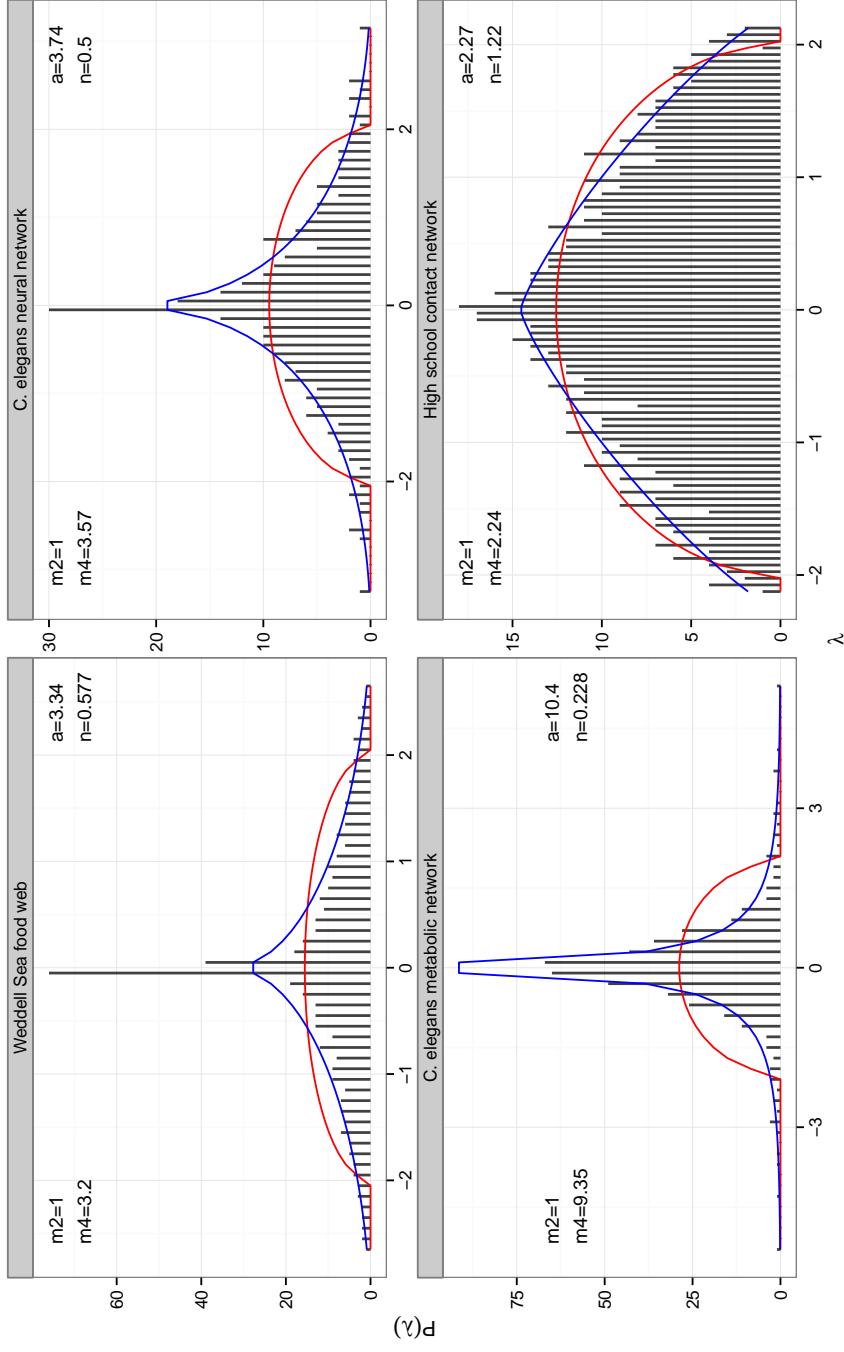


Figure S8: As main text Figure 1, but using networks of biological interest.

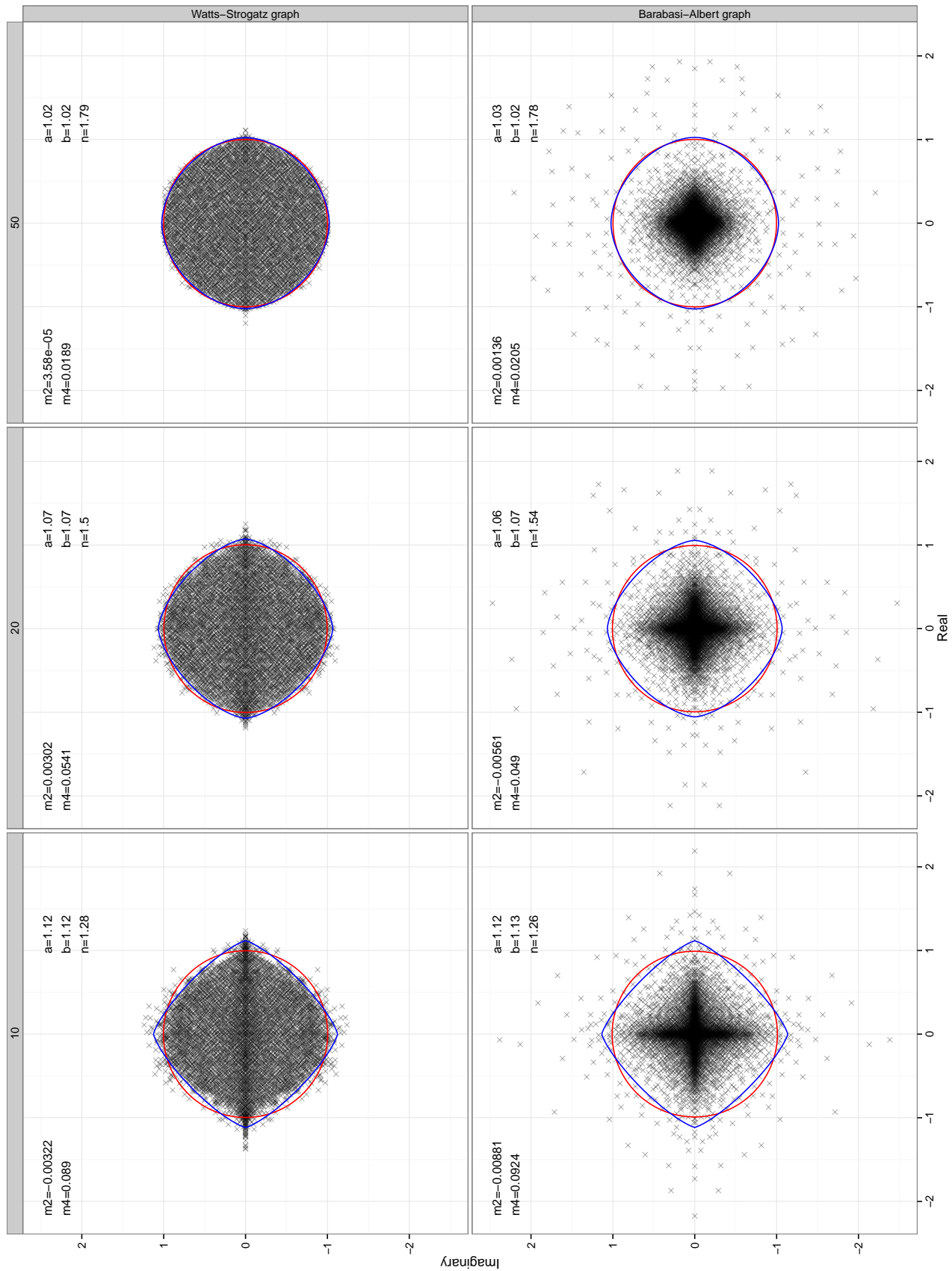


Figure S9: As main text Figure 2, but using different models to construct the networks.

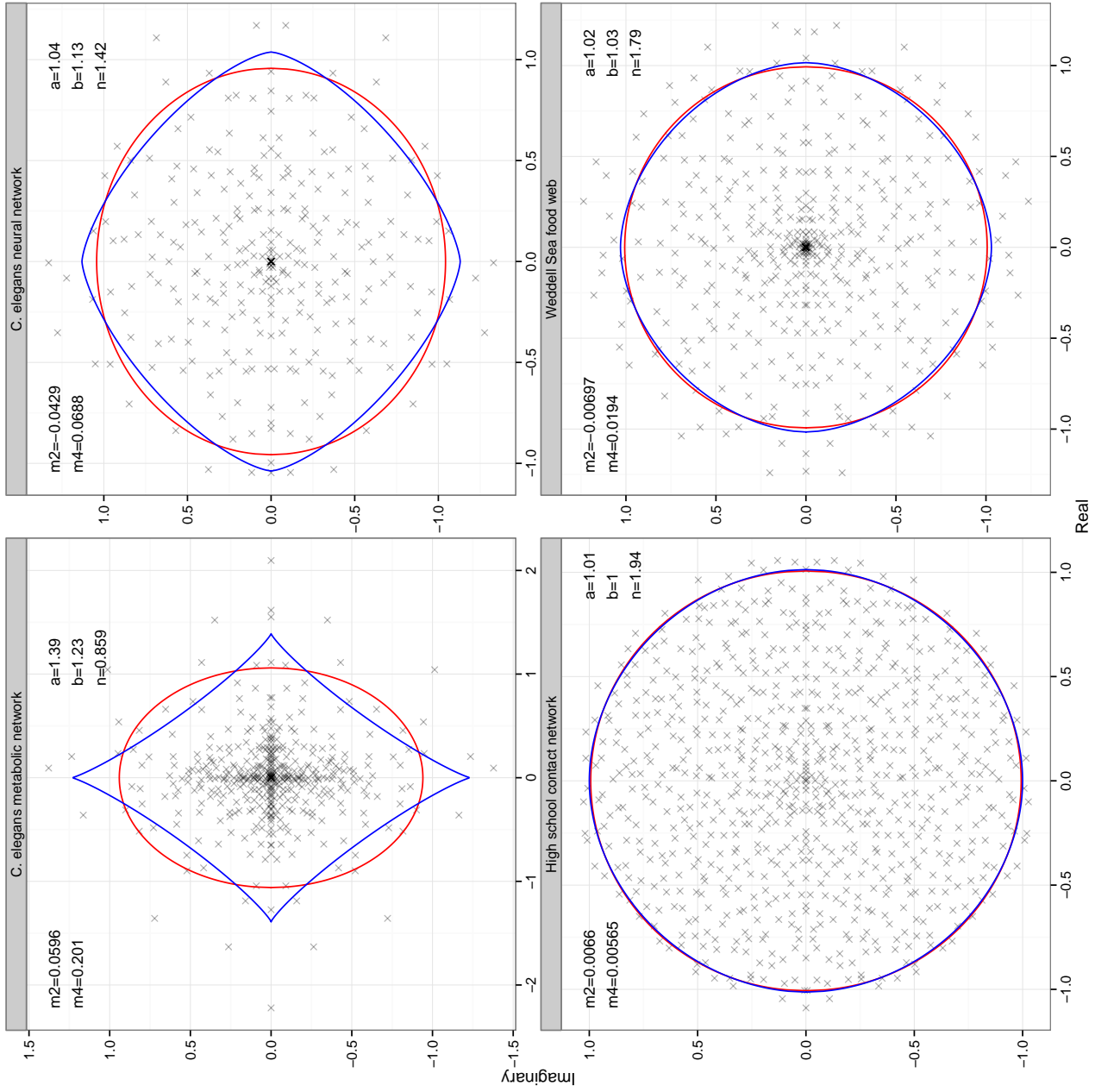


Figure S10: As main text Figure 2, but using networks of biological interest.



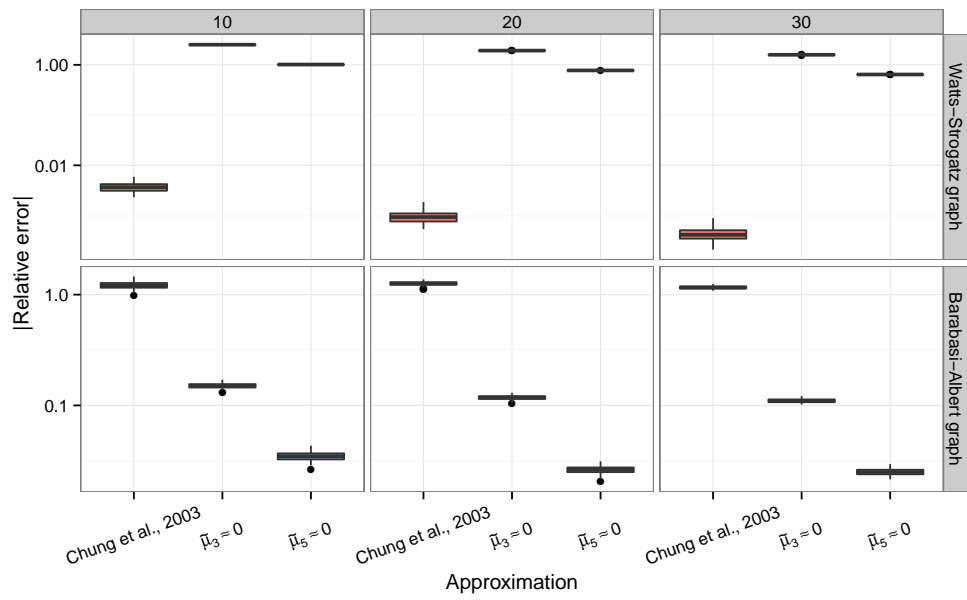


Figure S11: As main text Figure 4, but using different models.

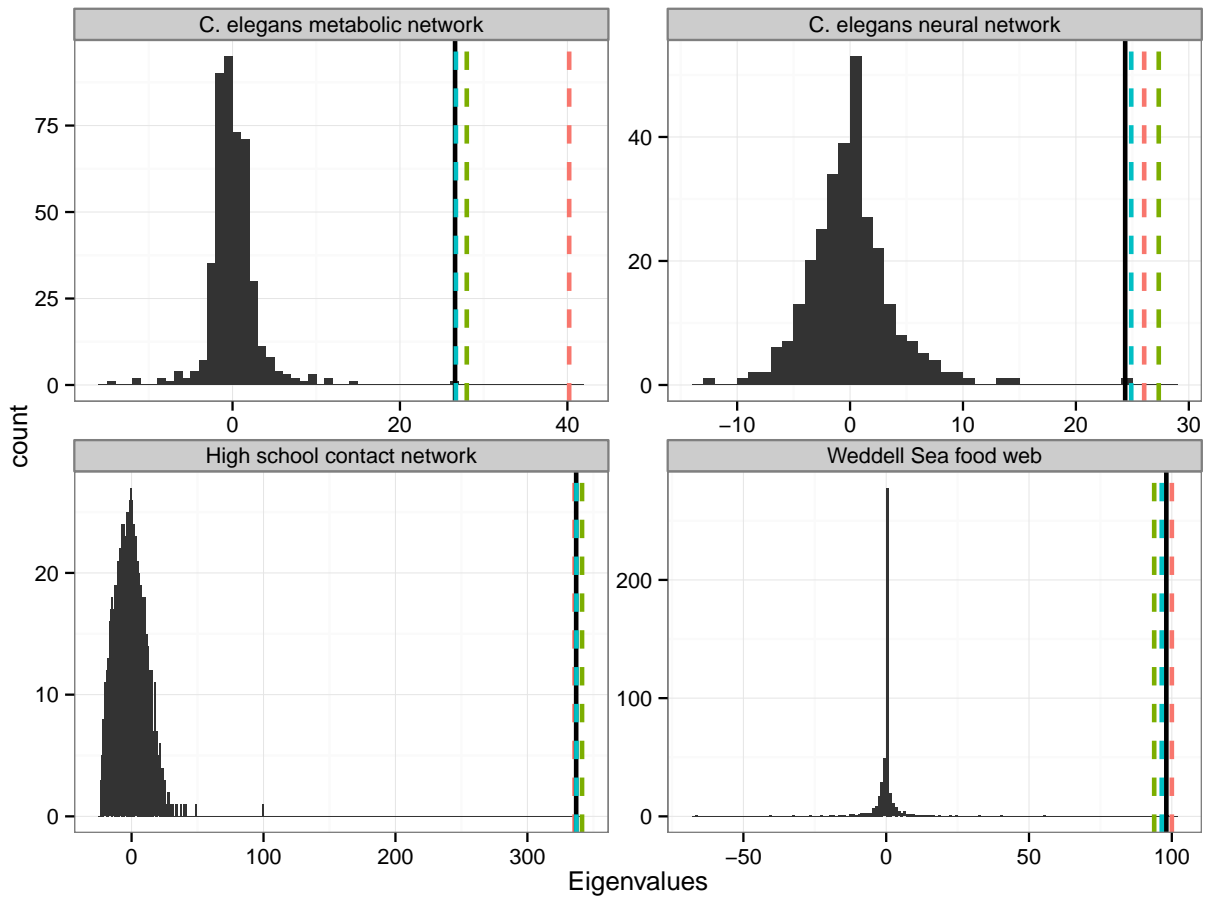


Figure S12: *The spectrum of the adjacency matrix of four networks of biological interest. The solid black line marks the value of  $\lambda_1$ . The dashed lines represent the approximations of Chung et al. (red) and those obtained by setting  $\tilde{\mu}_3 \approx 0$  (green) and  $\tilde{\mu}_5 \approx 0$  (turquoise).*

## References

- [1] Allesina, S. and Tang, S. Stability criteria for complex ecosystems. *Nature* **483**(7388), 205–208 (2012).
- [2] Barahona, M. and Pecora, L. M. Synchronization in small-world systems. *Physical Review Letters* **89**(5), 054101 (2002).
- [3] Pastor-Satorras, R. and Vespignani, A. Epidemic spreading in scale-free networks. *Physical Review Letters* **86**(14), 3200 (2001).
- [4] Chakrabarti, D., Wang, Y., Wang, C., Leskovec, J., and Faloutsos, C. Epidemic thresholds in real networks. *ACM Transactions on Information and System Security (TISSEC)* **10**(4), 1 (2008).
- [5] Youssef, M. and Scoglio, C. An individual-based approach to SIR epidemics in contact networks. *Journal of Theoretical Biology* **283**(1), 136–144 (2011).
- [6] Li, C., van de Bovenkamp, R., and Van Mieghem, P. Susceptible-Infected-Susceptible model: A comparison of N-intertwined and heterogeneous mean-field approximations. *Physical Review E* **86**(2), 026116 (2012).
- [7] Diekmann, O., Heesterbeek, J., and Roberts, M. The construction of next-generation matrices for compartmental epidemic models. *Journal of The Royal Society Interface* **7**(47), 873–885 (2010).
- [8] Bryan, K. and Leise, T. The \$25,000,000,000 eigenvector: The linear algebra behind Google. *SIAM Review* **48**(3), 569–581 (2006).
- [9] Wigner, E. P. On the distribution of the roots of certain symmetric matrices. *The Annals of Mathematics* **67**(2), 325–327 (1958).
- [10] Girko, V. Circular law. *Theory of Probability & Its Applications* **29**(4), 694–706 (1985).
- [11] Terras, A. *Zeta Functions of Graphs: a Stroll through the Garden*. Cambridge University Press, (2011).
- [12] Farkas, I. J., Derényi, I., Barabási, A.-L., and Vicsek, T. Spectra of “real-world” graphs: Beyond the semicircle law. *Physical Review E* **64**(2), 026704 (2001).
- [13] Barabási, A.-L. and Albert, R. Emergence of scaling in random networks. *Science* **286**(5439), 509–512 (1999).
- [14] Newman, M. E. J. The structure and function of complex networks. *SIAM Review* **45**(2), 167–256 (2003).
- [15] Chung, F., Lu, L., and Vu, V. Spectra of random graphs with given expected degrees. *Proceedings of the National Academy of Sciences* **100**(11), 6313–6318 (2003).
- [16] Nadakuditi, R. R. and Newman, M. E. Spectra of random graphs with arbitrary expected degrees. *Physical Review E* **87**(1), 012803 (2013).
- [17] Ginibre, J. Statistical ensembles of complex, quaternion, and real matrices. *Journal of Mathematical Physics* **6**, 440 (1965).
- [18] Tao, T., Vu, V., and Krishnapur, M. Random matrices: Universality of ESDs and the circular law. *The Annals of Probability* **38**(5), 2023–2065 (2010).
- [19] Girko, V. L. The elliptic law. *Teoriya Veroyatnostei i ee Primeneniya* **30**, 640–651 (1985).
- [20] Sommers, H. J., Crisanti, A., Sompolinsky, H., and Stein, Y. Spectrum of large random asymmetric matrices. *Physical Review Letters* **60**(19), 1895–1898 (1988).
- [21] Naumov, A. Elliptic law for real random matrices. *arXiv:1201:1639* (2012).

- [22] Guhr, T., Müller-Groeling, A., and Weidenmüller, H. A. Random-matrix theories in quantum physics: common concepts. *Physics Reports* **299**(4), 189–425 (1998).
- [23] Backstrom, L., Boldi, P., Rosa, M., Ugander, J., and Vigna, S. Four degrees of separation. In *Proceedings of the 3rd Annual ACM Web Science Conference*, 33–42. ACM, (2012).
- [24] Molloy, M. and Reed, B. A critical point for random graphs with a given degree sequence. *Random Structures & Algorithms* **6**(2-3), 161–180 (1995).
- [25] Milo, R., Shen-Orr, S., Itzkovitz, S., Kashtan, N., Chklovskii, D., and Alon, U. Network motifs: simple building blocks of complex networks. *Science* **298**(5594), 824–827 (2002).
- [26] Erdős, P. and Rényi, A. On random graphs. *Publicationes Mathematicae Debrecen* **6**, 290–297 (1959).
- [27] Csardi, G. and Nepusz, T. The igraph software package for complex network research. *InterJournal Complex Systems* , 1695 (2006).
- [28] R Core Team. *R: A Language and Environment for Statistical Computing*. R Foundation for Statistical Computing, Vienna, Austria, (2012).
- [29] Das, K. C. and Kumar, P. Some new bounds on the spectral radius of graphs. *Discrete Mathematics* **281**(1), 149–161 (2004).
- [30] Watts, D. J. and Strogatz, S. H. Collective dynamics of small-world networks. *Nature* **393**(6684), 440–442 (1998).
- [31] Salathé, M., Kazandjieva, M., Lee, J. W., Levis, P., Feldman, M. W., and Jones, J. H. A high-resolution human contact network for infectious disease transmission. *Proceedings of the National Academy of Sciences* **107**(51), 22020–22025 (2010).
- [32] White, J. G., Southgate, E., Thomson, J. N., and Brenner, S. The Structure of the Nervous System of the Nematode *Caenorhabditis elegans*. *Philosophical Transactions of the Royal Society of London. B, Biological Sciences* **314**(1165), 1–340 (1986).
- [33] Duch, J. and Arenas, A. Community detection in complex networks using extremal optimization. *Physical Review E* **72**(2), 027104 (2005).
- [34] Jacob, U. *Trophic dynamics of Antarctic shelf ecosystems: food webs and energy flow budgets*. PhD thesis, Bremen, Univ., Diss., 2005, (2005).